Group 5 *ansa*-Metallocenes: Structural and Dynamic Properties of Tetrahydroborate Complexes

Stephen L. J. Conway, Linda H. Doerrer, and Malcolm L. H. Green*

Inorganic Chemistry Laboratory, South Parks Road, Oxford, OX1 3QR, U.K.

Michael A. Leech

Chemical Crystallography Laboratory, 9 Parks Road, Oxford, OX1 3PD, U.K.

Received October 12, 1999

The new compounds [Nb{(η-C_5H_4)X(η-C_5H_4)}Cl_2] (X = CEt_2 **1a**, C(C_5H_{10}) **1b**, C_2Me_4 **1c**), [Nb{(η-$C_5H_3{}^tBu$)C_2Me_4(η-$C_5H_3{}^tBu$)}Cl_2] **1d**, [Nb{(η-C_5H_4)X(η-C_5H_4)}(η^2-BH_4)] (X = CEt_2 **2a***, C(C_5H_{10}) **2b**, C_2Me_4 **2c***, $SiMe_2$ **2e***), [Nb{(η-$C_5H_3{}^tBu$)C_2Me_4(η-$C_5H_3{}^tBu$)}(η^2-BH_4)] (**2d***), [Nb{(η-C_5H_4)X(η-C_5H_4)}(η^2-BD_4)] (X = C_2Me_4 **3c**, CMe_2 **4**), and [V{(η-C_5H_4)C_2Me_4(η-C_5H_4)}(η^2-BH_4)] (**5***) have been prepared. The asterisk indicates the crystal structure has been determined. The hydrogen scrambling processes in the tetrahydroborate complexes **2a**−**e,** **3c**, **4**, **5,** and [Nb{(η-C_5H_4)CMe_2(η-C_5H_4)}(η^2-BH_4)] have been studied. The free energy barrier $\Delta G^{\ddagger}$ to bridge-terminal hydrogen exchange is considerably reduced when the bridging unit imposes significant structural changes in the metallocene.

Introduction

It is well established that the presence of an *ansa*-bridge between the η-cyclopentadienyl ligands of metallocene complexes can have a profound effect on the reactivity and electronic properties of these compounds.[1−5] Varying the bridging unit is a simple yet powerful method of studying fundamental structure−reactivity relationships in organotransition metal chemistry.

We have recently described the preparation and reactivity of a number of *ansa*-metallocenes of group 6 metals,[1,2] as well as some preliminary investigations into the corresponding chemistry of *ansa*-metallocenes of niobium.[6] A significant number of group 5 *ansa*-metallocenes are now known, and their reactivity has been studied, particularly imido species of the type [M{(η-C_5H_4)CMe_2(η-C_5H_4)}(NR)Cl] (M = Nb, Ta, R = ^{t}Bu,[7] 2,6-$Pr_2C_6H_4$ [8]) and the dichloride complexes [M{(η-C_5R_4)X(η-C_5R_4)}Cl_2].[9]

The chemistry of metallocenes bearing the tetrahydroborate ligand BH_4 has been extensively studied.[10,11] The tetrahydroborate ligand displays multihapto coordination, of which the most common mode of bonding is bidentate M-μ^2-H_2BH_2 ligation. Exchange between the bridging and terminal hydrogens of the bidentate BH_4 unit is facile. In certain cases such as [M(η-C_5H_5)$_2$(η^2-BH_4)] (M = Nb, V) the free energy barrier $\Delta G^{\ddagger}$ to bridge-terminal hydrogen exchange is sufficiently large that the fluxional behavior becomes slow on the NMR time scale.[12]

We herein describe the preparation of new *ansa*-metallocenes of group 5 and a study of the structural and dynamic properties of the tetrahydroborate derivatives.

Results and Discussion

Synthesis and Characterization. We have previously reported the preparation of [Nb{(η-C_5H_4)CMe_2(η-C_5H_4)}Cl_2] via the addition of a suspension of [K_2(C_5H_4)-CMe_2(C_5H_4)] in THF to a suspension of $NbCl_4$·2THF in THF.[6] In an analogous procedure the compound [Nb{(η-C_5H_4)CEt_2(η-C_5H_4)}Cl_2] (**1a**) was prepared by the reaction between $NbCl_4$·2THF and [Li_2(C_5H_4)CEt_2(η-C_5H_4)]. The analytical and spectroscopic data for the compound **1a** and all other new compounds described are given in Table 1.

For the dichloride compounds [Nb{(η-C_5H_4)X(η-C_5H_4)}-Cl_2] (X = C(C_5H_{10}) **1b**, X = C_2Me_4 **1c**) and [Nb{(η-$C_5H_3{}^t$-Bu)C_2Me_4(η-$C_5H_3{}^t$Bu)}Cl_2] (**1d**) higher yields were obtained via a procedure modified from that used for the preparation of *ansa*-metallocenes of group 6. The com-

* Corresponding author. E-mail: malcolm.green@chem.ox.ac.uk.

(1) Chernega, A.; Cook, J.; Green, M. L. H.; Labella, L.; Simpson, S. J.; Souter, J.; Stephens, A. H. H. *J. Chem. Soc., Dalton Trans.* **1997**, 3225−3243.

(2) Conway, S. L. J.; Dijkstra, T.; Doerrer, L. H.; Green, J. C.; Green, M. L. H.; Stephens, A. H. H. *J. Chem. Soc., Dalton Trans.* **1998**, 2689−2695.

(3) Smith, J. A.; Brintzinger, H. H. *J. Organomet. Chem.* **1981**, *218*, 159−167.

(4) Churchill, D.; Shin, J. H.; Hascall, T.; Hahn, J. M.; Bridgewater, B. M.; Parkin, G. *Organometallics* **1999**, *18*, 2403−2406.

(5) Green, J. C. *Chem. Soc. Rev.* **1998,** 263−271, and references therein.

(6) Bailey, N. J.; Green, M. L. H.; Leech, M. A.; Saunders, J. F.; Tidswell, H. M. *J. Organomet. Chem.* **1997**, *538*, 111−118.

(7) Bailey, N. J.; Cooper, J. A.; Gailus, H.; Green, M. L. H.; James, J. T.; Leech, M. A. *J. Chem. Soc., Dalton Trans.* **1997**, 3579−3584.

(8) Herrmann, W. A.; Baratta, W.; Herdtweck, E. *J. Organomet. Chem.* **1997**, *541*, 445−460.

(9) For leading articles see for example: (a) Dorer, B.; Prosenc, M. H.; Rief, U.; Brintzinger, H. H. *J. Organomet. Chem.* **1992**, *427*, 245−255. (b) Shin, J. H.; Parkin, G. *J. Chem. Soc., Chem. Commun.* **1999**, 887−888. (c) Huttenloch, M. E.; Dorer, B.; Rief, U.; Prosenc, M.-H.; Schmidt, K.; Brintzinger, H. H. *J. Organomet. Chem.* **1997**, *541*, 219−232.

(10) Johnson, P. L.; Cohen, S. A.; Marks, T. J.; Williams, J. M. *J. Am. Chem. Soc.* **1978**, *100*, 2709.

(11) Green, M. L. H.; Wong, L.-L. *J. Chem. Soc., Dalton Trans.* **1989**, 2133−2138.

(12) Bell, R. A.; Cohen, S. A.; Doherty, N. M.; Threlkel, R. S.; Bercaw, J. E. *Organometallics* **1986**, *5*, 972−975.

10.1021/om990810n CCC: $19.00
Publication on Web 01/18/2000

Table 1. Analytical and Spectroscopic Data

compound and analysis[a]	spectroscopic data[b]
1a, [Nb{(η-C_5H_4)CEt_2(η-C_5H_4)}Cl_2] purple C, 49.7 (49.8); H, 5.3 (5.0)	mass (FAB): *m/z* 361 (M^+), 326 ($M^+ - Cl$) ESR: 10 lines, $g_{iso} = 1.998$, $\lvert a^{93}Nb\rvert_{iso} = 94$ G
1b, [Nb{(η-C_5H_4)C(C_5H_{10})(η-C_5H_4)}Cl_2] brown C, 51.7 (51.4); H, 5.5 (4.9)	mass (FAB): *m/z* 373 (M^+), 338 ($M^+ - Cl$), 303 ($M^+ - 2Cl$) ESR: 10 lines, $g_{iso} = 1.994$, $\lvert a^{93}Nb\rvert_{iso} = 95$ G
1c, [Nb{(η-C_5H_4)C_2Me_4(η-C_5H_4)}Cl_2] brown C, 50.8 (51.1); H, 5.1 (5.4); Cl, 19.4 (18.9)	mass (FAB): *m/z* 375 (M^+), 340 ($M^+ - Cl$) ESR: 10 lines, $g_{iso} = 2.008$, $\lvert a^{93}Nb\rvert_{iso} = 110$ G
1d, [Nb{(η-$C_5H_3{}^tBu$)C_2Me_4(η-$C_5H_3{}^tBu$)}Cl_2] brown C, 58.4 (59.0); H, 7.4 (7.4)	mass (FAB): *m/z* 487 (M^+), 452 ($M^+ - Cl$) ESR: 10 lines, $g_{iso} = 1.987$, $\lvert a^{93}Nb\rvert_{iso} = 112$ G
2a, [Nb{(η-C_5H_4)CEt_2(η-C_5H_4)}(η^2-BH_4)] green C, 57.8 (58.9); H, 7.7 (7.3); B, 3.0 (3.5)	^{1}H:[c] 5.67 [4H, m, C_5H_4], 4.59 [4H, m, C_5H_4], 0.44 [6H, t, CH_2CH_3], 0.31 [4H, q, CH_2CH_3], −3.38 [4H, br, BH_4] ^{13}C {^{1}H}:[c] 106.2 [s, C_5H_4], 79.7 [s, C_5H_4], 77.0 [s, C_5H_4, C_{ipso}], 20.7 [s, CH_2CH_3], 6.1 [s, CH_2CH_3] ^{11}B:[c] 20.5 [quintet, $J = 85$ Hz, BH_4] IR:[d] 2442 ν(B−H_t), 2395 ν(B−H_t), 1715 ν(B−H_b), 1703 ν(B−H_b)
2b, [Nb{(η-C_5H_4)C(C_5H_{10})(η-C_5H_4)}(η^2-BH_4)] dark green C, 59.7 (60.4); H 6.7 (7.0)	^{1}H:[c] 5.70 [4H, m, C_5H_4], 4.61 [4H, m, C_5H_4], 1.11 [4H, m, C(C_5H_{10})], 0.38 [4H, m, C(C_5H_{10})], 0.28 [2H, m, C(C_5H_{10})], −3.37 [4H, br, BH_4] ^{13}C {^{1}H}:[c,e] 106.4 [s, C_5H_4], 79.5 [s, C_5H_4], 37.9 [s, C(C_5H_{10})], 30.6 [s, C(C_5H_{10})], 30.2 [s, C(C_5H_{10})], 26.2 [s, C(C_5H_{10})] ^{11}B:[c] 18.2 [quintet, $J = 90$ Hz, BH_4] IR:[d] 2417 ν(B−H_t), 2402 ν(B−H_t), 1705 ν(B−H_b), 1695 ν(B−H_b)
2c, [Nb{(η-C_5H_4)C_2Me_4(η-C_5H_4)}(η^2-BH_4)] green C, 60.1 (60.0); H, 7.8 (7.6); B, 3.3 (3.4)	^{1}H:[c,f] 5.66 [4H, m, C_5H_4], 5.52 [4H, m, C_5H_4], 0.36 [12H, s, C_2Me_4], ^{13}C {^{1}H}:[c,e] 103.1 [s, C_5H_4], 85.2 [s, C_5H_4], 43.8 [s, C_2Me_4], 26.4 [s, C_2Me_4] ^{11}B:[c] 26.9 [quintet, $J = 86$ Hz, BH_4] IR:[d] 2465 ν(B−H_t), 2427 ν(B−H_t), 1712 ν(B−H_b), 1661 ν(B−H_b)
2d, [Nb{(η-$C_5H_3{}^tBu$)C_2Me_4(η-$C_5H_3{}^tBu$)}(η^2-BH_4)] green C, 66.0 (66.7); H, 9.5 (9.3); B 2.4 (2.5)	^{1}H:[c,f] *rac*-**2d** 6.22 [2H, dd, C_5H_3], 5.37 [2H, t, C_5H_4], 5.26 [2H, t, C_5H_4], 1.40 [9H, s, ^{t}Bu], 0.53 [6H, s, C_2Me_4],], 0.49 [6H, s, C_2Me_4] meso-**2d** 6.36 [2H, dd, C_5H_3], 5.13 [2H, t, C_5H_4], 5.12 [2H, t, C_5H_4], 1.31 [9H, s, ^{t}Bu], 0.48 [6H, s, C_2Me_4],], 0.40 [6H, s, C_2Me_4] ^{13}C {^{1}H}[c]: *rac*-**2d** 99.8 [s, C_5H_3], 84.7 [s, C_5H_3], 80.4 [s, C_5H_3], 44.0 [s, C_{ipso}] 31.9 [s, C(CH_3)], 28.8 [s, C_2Me_4], 23.9 [s, C_2Me_4] meso-**2d**[e] 99.6 [s, C_5H_3], 87.1 [s, C_5H_3], 83.6 [s, C_5H_3], 44.4 [s, $C(CH_3)$] 32.1 [s, C(CH_3)], 27.1 [s, C_2Me_4], 21.0 [s, C_2Me_4] ^{11}B:[c] 26.9 [quintet, $J = 86$ Hz, BH_4] IR:[d] 2467 ν(B−H_t), 2430 ν(B−H_t), 1690 ν(B−H_b), 1666 ν(B−H_b)
2e, [Nb{(η-C_5H_4)$SiMe_2$(η-C_5H_4)}(η^2-BH_4)] green C, 49.3 (49.0); H, 6.2 (6.2); B, 3.4 (3.7)	^{1}H:[c,f] 6.03 [4H, m, C_5H_4], 5.16 [4H, m, C_5H_4], −0.62 [6H, s, $SiMe_2$] ^{13}C {^{1}H}:[c] 111.5 [s, C_5H_4], 87.1 [s, C_5H_4], 74.5 [s, C_5H_4, C_{ipso}], −6.8 [s, $SiMe_2$] ^{11}B:[c] 26.8 [quintet, $J = 86$ Hz, BH_4] mass (FAB): *m/z* 296 ($M^+ + 2$), 279 ($M^+ - BH_4$) IR:[d] 2460 ν(B−H_t), 2410 ν(B−H_t), 1703 ν(B−H_b), 1652 ν(B−H_b)
3c, [Nb{(η-C_5H_4)C_2Me_4(η-C_5H_4)}(η^2-BD_4)] green C, 59.1 (59.3); H/D, 8.7 (8.8); B, 3.3 (3.3)	^{1}H:[c] 5.70 [4H, m, C_5H_4], 5.59 [4H, m, C_5H_4], 0.37 [12H, s, C_2Me_4] ^{2}H:[g] −4.91 [br, s, BD_4] ^{13}C {^{1}H}:[c,e]104.0 [s, C_5H_4], 85.7 [s, C_5H_4], 44.1 [s, C_2Me_4], 26.8 [s, C_2Me_4] ^{11}B:[c] 25.5 [br s, BD_4] IR:[d] 1880 ν(B−D_t), 1769 ν(B−D_t), 1261 ν(B−D_b)
4, [Nb{(η-C_5H_4)CMe_2(η-C_5H_4)}(η^2-BD_4)] green C, 55.0 (55.4); H/D 8.0 (7.9)	^{1}H:[c] 5.65 [4H, m, C_5H_4], 4.58 [4H, m, C_5H_4], 0.10 [6H, s, CMe_2] ^{2}H:[g] −2.99 [br, s, BD_4] ^{13}C {^{1}H}:[c,e] 106.3[s, C_5H_4], 79.5 [s, C_5H_4], 30.2 [s, CMe_2] 20.9 [s, CMe_2] ^{11}B: 21.6 [br, s, BD_4] IR:[d] 1860 ν(B−D_t), 1790 ν(B−D_t), 1270 ν(B−D_b)
5, [V{(η-C_5H_4)C_2Me_4(η-C_5H_4)}(η^2-BH_4)] purple C, 68.9 (69.1); H, 8.5 (8.7)	^{1}H:[c] 6.47 [4H, m, C_5H_4], 4.74 [4H, m, C_5H_4], 0.25 [12H, s, C_2Me_4], −9.10 [4H, br d, $J = 90$ Hz, BH_4] ^{13}C {^{1}H}:[c,e]108.1 [s, C_5H_4], 88.1 [s, C_5H_4], 42.9 [s, C_2Me_4], 26.1 [s, C_2Me_4] ^{11}B: 26.5 [quintet, $J = 86$ Hz, BH_4] mass (FAB): *m/z* 278 (6, M^+), 263 (47, $M^+ - BH_4$) IR:[d] 2450 ν(B−H_t), 2410 ν(B−H_t), 1750 ν(B−H_b), 1627 ν(B−H_b)

[a] Required values given in parentheses. [b] NMR data recorded at room temperature are given as chemical shift (δ) [multiplicity, relative intensity, assignment, *J*/Hz]. Where necessary assignments were confirmed using ^{1}H−^{1}H and ^{1}H−^{13}C shift correlation experiments. [c] In $C_6D_5CD_3$. [d] IR data (cm^{-1}) determined in Nujol Mulls. B−H/D_t and B−H/D_b stretching frequencies assigned by analogy to [Nb(η-C_5H_5)$_2$(η^2-BH_4)] and [V(η-C_5H_5)$_2$(η^2-BD_4)].[18] [e] C_{ipso} was not located. [f] Resonances due to BH_4 protons were not located at 298 K. [g] In C_7H_8.

pound **1b** was prepared by stirring $NbCl_4$·2THF and [Li_2(C_5H_4)C(C_5H_{10})(C_5H_4)] in diethyl ether for 3 days. The compounds **1c** and **1d** were prepared in an analogous manner by the reaction of $NbCl_4$·2THF with [(MgCl)$_2$(C_5H_4)C_2Me_4(C_5H_4)·4THF] for **1c** and [(MgCl)$_2$-{($C_5H_3{}^tBu$)C_2Me_4($C_5H_3{}^tBu$)}·4THF] for **1d**.

The ESR spectra of the dichloride compounds **1a**−**d** showed the expected 10-line pattern for an unpaired electron coupled to the ^{93}Nb ($I = 9/2$) nucleus. The hyperfine coupling constant $\lvert a^{93}Nb\rvert_{iso}$ is reduced for the single carbon-bridged species **1a** ($\lvert a^{93}Nb\rvert_{iso} = 94$ G) and **1b** ($\lvert a^{93}Nb\rvert_{iso} = 95$ G) compared to that reported for the

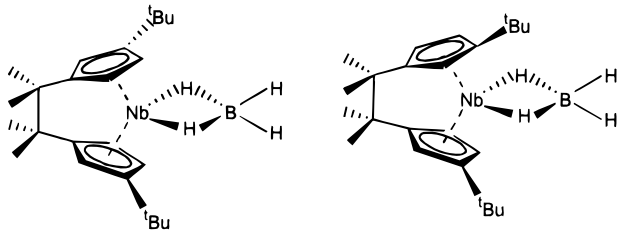

Figure 1. Rac- and meso-isomers of [Nb{(η-$C_5H_3{}^tBu$)C_2Me_4(η-$C_5H_3{}^tBu$)}(η^2-BH_4)], **2d**.

nonbridged compound [Nb(η-C_5H_5)$_2Cl_2$] ($|a^{93}Nb|_{iso}$ = 116 G).[13] The values of $|a^{93}Nb|_{iso}$ for the ethylene-bridged compounds **1c** ($|a^{93}Nb|_{iso}$ = 110 G) and **1d** ($|a^{93}Nb|_{iso}$ = 112 G) are close to that seen in the analogous nonbridged compound.

Otero has described the synthesis of [Nb{(η-C_5H_4)$SiMe_2$(η-C_5H_4)}Cl_2] by the reaction of $NbCl_4$·2THF with [Tl_2(C_5H_4)$SiMe_2$(C_5H_4)] in THF.[14] The thallium reagent rather than the lithium reagent was employed because the reaction between $NbCl_4$·2THF and [Li_2-(C_5H_4)$SiMe_2$(C_5H_4)] in THF gave diminished yields, which was attributed to reduction processes. However, using the lithium reagent in a reaction analogous to that used to prepare the compounds **1b**−**d** gives [Nb{(η-C_5H_4)$SiMe_2$(η-C_5H_4)}Cl_2] (**1e)** in 36% yield. This yield is typical for the synthesis of *ansa*-metallocenes of group 5 and group 6.

Treatment of the compound **1a** with lithium borohydride in DME at room temperature gives green, air-sensitive crystals of the compound [Nb{(η-C_5H_4)CEt_2(η-C_5H_4)}(η^2-BH_4)] (**2a**). The IR spectrum of the compound **2a** shows two bands in the terminal B−H region at 2442 and 2395 cm^{-1} and two bands in the bridging M−H−B region at 1715 and 1703 cm^{-1}, consistent with a bidentate η^2-BH_4 binding mode. The room-temperature ^1H NMR spectrum of **2a** shows a broad singlet centered at δ −3.3 ppm due to the protons of the tetrahydroborate unit. That only one resonance is observed for the tetrahydroborate hydrogens implies that the exchange between bridging and terminal hydrogens is fast at room temperature on the NMR time scale.

The compounds [Nb{(η-C_5H_4)X(η-C_5H_4)}(η^2-BH_4)] (X = C(C_5H_{10}) **2b**, C_2Me_4 **2c**, $SiMe_2$ **2e**), [Nb{(η-$C_5H_3{}^tBu$)-C_2Me_4(η-$C_5H_3{}^tBu$)}(η^2-BH_4)] (**2d**), and [Nb{(η-C_5H_4)X-(η-C_5H_4)}(η^2-BD_4)] (X = C_2Me_4 **3c**, CMe_2 **4**) were prepared in an analogous manner and fully characterized. For the compound **2d** rac- and meso-isomers were obtained in 3:2 ratio. The rac-isomer could be isolated from this mixture by recrystallization. The rac- and meso-isomers of **2d** are shown in Figure 1. The vanadocene complex [V{(η-C_5H_4)C_2Me_4(η-C_5H_4)}(η^2-BH_4)] (**5**) was prepared by the action of sodium borohydride on a solution of [V{(η-C_5H_4)C_2Me_4(η-C_5H_4)}Cl_2] in DME at low temperature.

The molecular structures of the compounds **2a**, **2c**, *rac*-**2d**, **2e**, and **5** were determined by X-ray crystallography and are shown in Figures 2−6. Selected bond distances and angles are given in Table 2.

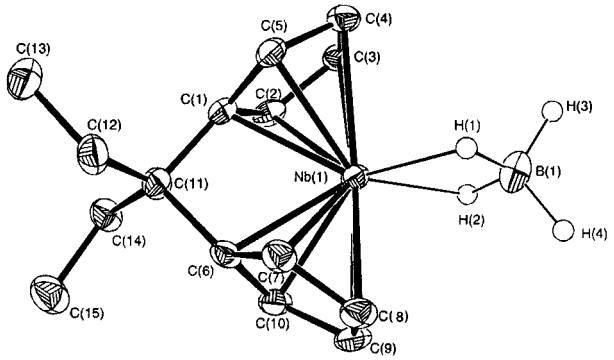

Figure 2. Molecular structure of [Nb{(η-C_5H_4)CEt_2(η-C_5H_4)}(η^2-BH_4)], **2a**. Hydrogen atoms attached to carbon atoms are omitted for clarity.

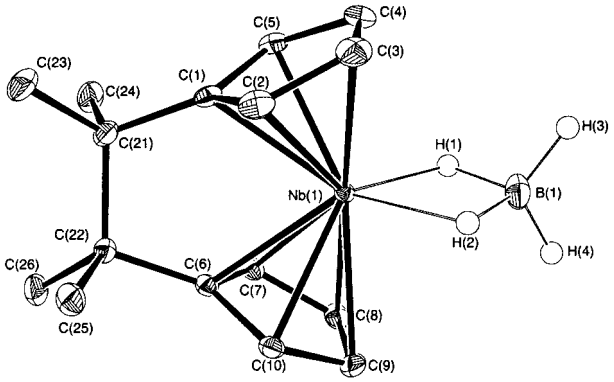

Figure 3. Molecular structure of [Nb{(η-C_5H_4)C_2Me_4(η-C_5H_4)}(η^2-BH_4)], **2c**. Hydrogen atoms attached to carbon atoms are omitted for clarity.

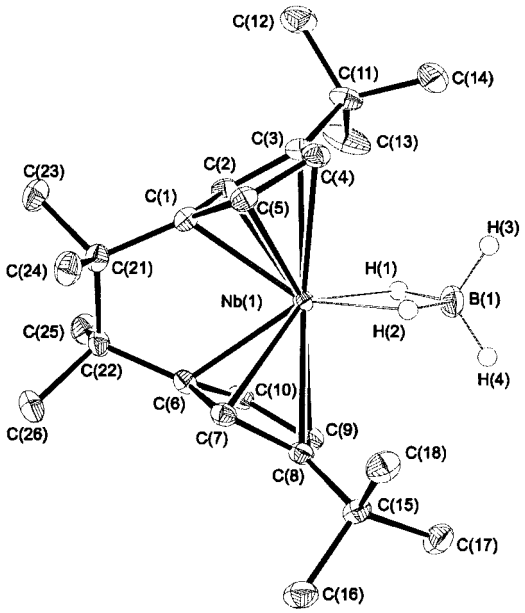

Figure 4. Molecular structure of *rac*-[Nb{(η^5-$C_5H_3{}^tBu$)-C_2Me_4(η^5-$C_5H_3{}^tBu$)}(η^2-BH_4)], **2d**. Hydrogen atoms attached to carbon atoms are omitted for clarity.

The molecular structures confirm the assignment of a bidentate η^2-BH_4 binding mode. The structures provide a good illustration of how the geometrical consequences of an *ansa*-bridge depend on the nature of the bridging unit. Geometric parameters relevant to *ansa*-metallocenes are defined in Figure 7. Of particular note

(13) Benoit, R. L.; Lam, S. Y. *J. Am. Chem. Soc.* **1974**, *24*, 7385−7387.

(14) Antiñolo, A.; Martinez-Ripoll, M.; Mugnier, Y.; Otero, A.; Prashar, S.; Rodriguez, A. M. *Organometallics* **1996**, *15*, 3241−3243.

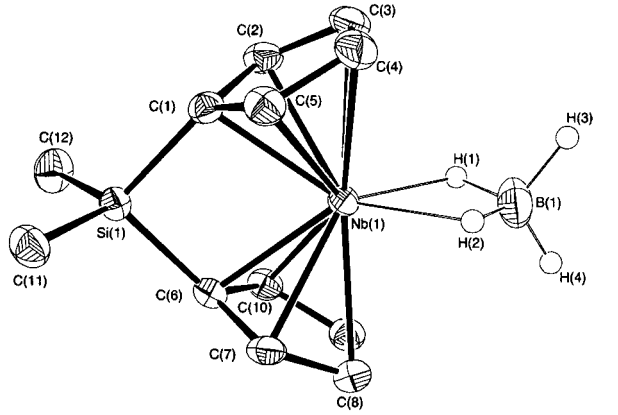

Figure 5. Molecular structure of [Nb{(η-C_5H_4)$SiMe_2$(η-C_5H_4)}(η^2-BH_4)], **2e**. Hydrogen atoms attached to carbon atoms are omitted for clarity.

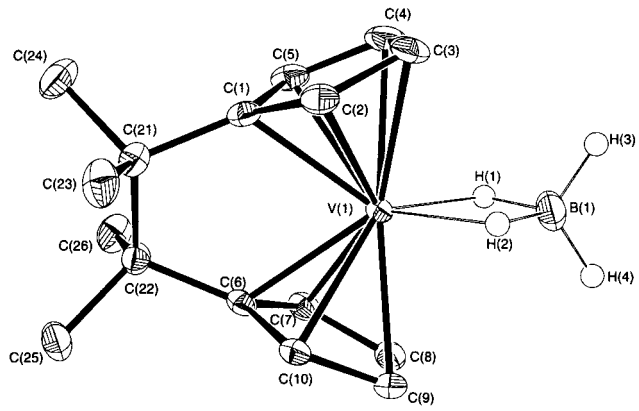

Figure 6. Molecular structure of [V{(η-C_5H_4)C_2Me_4(η-C_5H_4)}(η^2-BH_4)], **5**. Hydrogen atoms attached to carbon atoms are omitted for clarity.

in the compounds **2a**, **2c**−**e**, and **5** is the change in bending angles β and γ. The bending angle β in [Nb(η-C_5H_5)$_2$(η-BH_4)] is reported as 127.1°.[15] For the methylene-bridged species **2a** this is substantially reduced to 115.6°.

As has been observed in other series of *ansa*-metallocenes, the presence of a silicon- or ethylene-bridge appears to alter the bending angles in a similar manner[2,16] and the bending angles in **2c**−**e** do not vary significantly from those in the nonbridged analogue [Nb(η-C_5H_5)$_2$(η^2-BH_4)]. As expected, the bending angle β in the vanadium compound **5** is larger than in the corresponding niobium compound **2c**. The decrease in the bending angle β is correlated to a shortening of the distance between the *ipso*-carbons of the cyclopentadienyl rings. The C_{ipso}−C_{ipso} distance is shortest in **2a** (2.29 Å), whereas the other niobium compounds show longer C_{ipso}−C_{ipso} distances (2.66−2.70 Å). In the single-atom-bridged species **2a** and **2e** there is a large deviation from planarity at the *ipso*-carbon, as evidenced by values of ϕ (Figure 7), ca. 17.2° for **2a** and ca. 20.6° for **2e**. The departure from planarity at the *ipso*-carbons in the ethylene-bridged species is much smaller, although in contrast to the single-atom-bridged compounds the *ipso*-carbon vector lies above the plane of the cyclopentadienyl rings, reflecting the steric demand of a two-carbon bridge. In **2c**, *rac*-**2d**, and **2e** the *ipso*-carbons and the carbons of the bridge are not coplanar, corresponding to a twisting of the bridging unit.

In the molecular structures determined, the bridging B−H_b bond lengths are greater than the terminal B−H_t bond lengths, consistent with covalent interaction between the metal and BH_4 ligand. This is also reflected in the B−H stretching frequencies, with the terminal B−H stretching frequencies found at higher energy than the bridging B−H stretching frequencies. Girolami described the use of the correlation between the average symmetric and antisymmetric stretching frequencies for the B−H_t and B−H_b bonds as a gauge of the M−BH_4 covalent interaction.[17] Figure 8 shows these parameters for the compounds **2a**−**e** and **5** and for the nonbridged species [Nb(η-C_5H_5)$_2$(BH_4)], [Nb(η-C_5Me_5)$_2$(BH_4)], and [V(η-C_5H_5)$_2$(BH_4)].[12,18] Although the comparison is somewhat crude, it can seen that there is a slight strengthening of the B−H_b bonds and weakening of the B−H_t bonds in the methylene-bridged species **2a** and **2b** relative to the nonbridged analogues, suggesting a reduced M−BH_4 covalent interaction. Theoretical studies on *ansa*-metallocenes show that as the bending angle β is reduced, two of the metal d-orbitals become more involved in metal−ring bonding and less available for bonding to other ligands.[5,19]

NMR Studies. The exchange between terminal and bridging hydrogens in the η^2-BH_4 ligand in the compounds **2a**−**e**, **3**−**5**, and [Nb{(η-C_5H_4)CMe_2(η-C_5H_4)}(η^2-BH_4)] was investigated by variable-temperature NMR spectroscopy. Fast and slow exchange was accessible for all compounds, thus allowing the calculation of the free energy barrier at the coalescence temperature T_c to terminal-bridging hydrogen exchange $\Delta G^{\ddagger}$.

Variable-temperature ^{1}H NMR spectra between 183 and 363 K for the ethylene-bridged compound **2c** in $C_6D_5CD_3$ are shown in Figure 9. At high temperature exchange is fast on the NMR time scale, and a single broad resonance is observed at δ −4.97 ppm. As temperature is decreased, this resonance broadens until coalescence occurs at $T_c = 308 \pm 3$ K, corresponding to a free energy barrier to exchange $\Delta G^{\ddagger} = 49.9 \pm 1$ kJ mol^{-1}.[20] Below the coalescence temperature T_c two singlets are observed at δ 5.3 and −14.9 ppm due to the terminal and bridging hydrogens of the η^2-BH_4 unit, respectively. These two resonances sharpen as the temperature is reduced.

The exchange processes for all the new tetrahydroborate species **2a**−**e**, **3c**, **4**, **5**, and [Nb{(η-C_5H_4)CMe_2(η-C_5H_4)}(η^2-BH_4)] were studied using variable-temperature NMR spectroscopy. The relevant spectral data for these compounds are summarized in Table 3.

The free energy barrier (at T_c) $\Delta G^{\ddagger}$ and the bending angle β for the compounds **2a**−**e**, **3**−**5**, [Nb{(η-C_5H_4)-CMe_2(η-C_5H_4)}(η^2-BH_4)], [Nb(η-C_5H_5)$_2$(η^2-BH_4)], [Nb(η-C_5Me_5)$_2$(η^2-BH_4)], and [V(η-C_5H_5)$_2$(η^2-BH_4)] are compared in Table 4.

(15) Kurillova, N. I.; Gusev, A. I.; Struchkov, Y. T. *Zh. Strukt. Khim.* **1974**, *15*, 718−722.
(16) Shaltout, R. M.; Corey, J. Y.; Rath, N. P. *J. Organomet. Chem.* **1995**, *503*, 205−212.
(17) Jensen, J. A.; Girolami, G. S. *Inorg. Chem.* **1989**, *28*, 2107−2113.
(18) Marks, T. J.; Kennelly, W. J. *J. Am. Chem. Soc.* **1975**, *97*, 1439−1443.
(19) Green, J. C.; Scottow, A. *N. J. Chem.* **1999**, *23*, 651−655.
(20) $\Delta G^{\ddagger}$ (kJ mol^{-1}) = $RT_c(22.96 + \ln(T_c/\Delta\nu)$.

Table 2. Selected Interatomic Distances (Å) and Angles (deg) for the Compounds 2a, 2c−e, and 5[a]

	2a	2c	2d	2e	5
$M-Cp^1_{cent}$	2.0076	2.0240	2.0493	2.0350	1.9050
$M-Cp^1_{av}$	2.344(4)	2.3584(14)	2.380(18)	2.365(4)	2.2552(17)
$M-Cp^2_{cent}$	2.0104	2.030	2.0478	2.0329	1.9029
$M-Cp^2_{av}$	2.347(4)	2.3644(14)	2.3796(18)	2.367(3)	2.2530(17)
M−C(1)	2.280(4)	2.3041(13)	2.299(3)	2.307(3)	2.2159(15)
M−C(3)	2.423(3)	2.4274(15)	2.497(3)	2.429(4)	2.2861(18)
$C_{ipso}-C_{ipso}$	2.22934	2.6835	2.6649	2.6991	2.5996
M−H(1)	2.04(6)	1.81(2)	1.89(5)	1.92(5)	1.76(3)
B−H(1)	1.25(6)	1.28(2)	1.17(5)	1.24(5)	1.18(3)
B−H(3)	1.16(7)	1.12(3)	1.10(5)	1.11(3)	1.06(3)
between Cp planes, α	64.4	52.2	55.3	52.8	47.7
$Cp^1_{norm}-M-Cp^2_{norm}$, β	115.6	127.8	124.7	127.2	132.3
$Cp^1_{cent}-M-Cp^2_{cent}$, χ	124.98	134.38	133.60	135.69	137.71
C_{ipso}−Cp plane, ϕ	17.2, 17.3	2.4, 2.6	4.8, 3.4	20.8, 20.4	2.0, 1.6
$C_{ipso}-X-C_{ipso}$, ϵ	97.2(3)			92.79(9)	

[a] Cp^1_{cent} = ring C(1)−C(5), Cp^2_{cent} = ring C(6)−C(10).

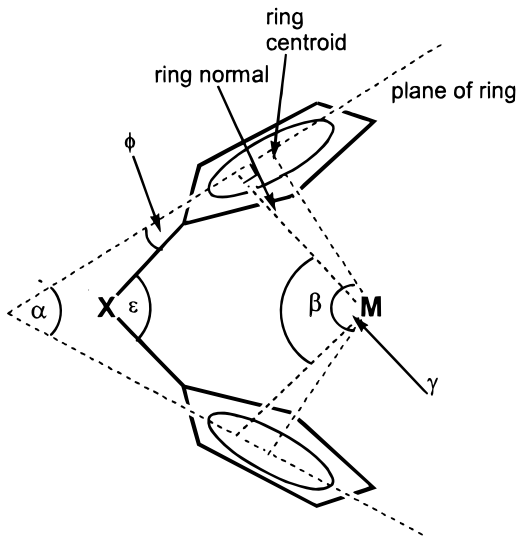

Figure 7. Geometric parameters in an *ansa*-metallocene. α = angle between the ring planes; β = angle between the normals to the ring planes; χ = ring centroid−metal−ring centroid angle; ϵ = angle between vectors from a bridging atom X to the *ipso*-carbons; ϕ = angle between *ipso*-carbon vector and the ring plane.

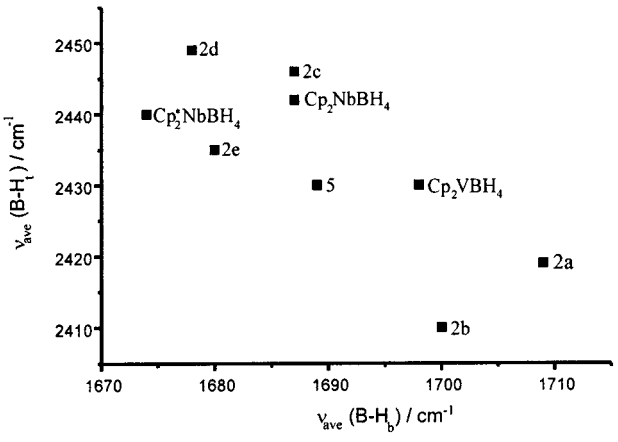

Figure 8. B−H stretching frequencies for compounds **2a**−**e**, **5,** and other group 5 metallocene tetrahydroborate complexes.

The barrier to exchange $\Delta G^{\ddagger}$ is reduced by around 25 kJ mol^{-1} for the methylene-bridged species [Nb{(η-C_5H_4)CMe_2(η-C_5H_4)}(η^2-BH_4)], **2a** and **2b**, relative to the

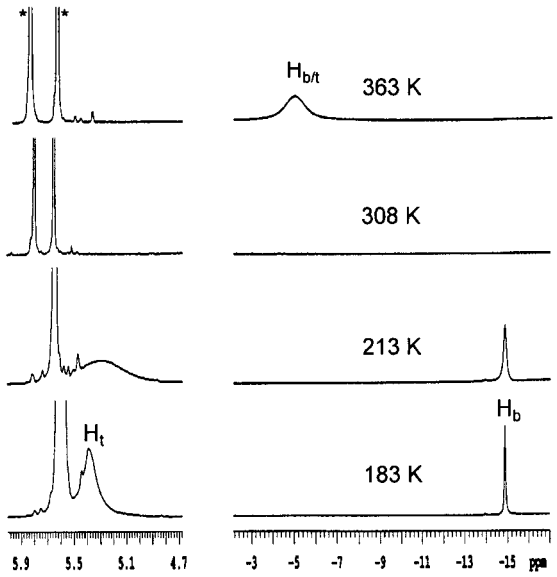

Figure 9. Partial variable-temperature 500 MHz ^{1}H NMR spectra of [Nb{(η-C_5H_4)C_2Me_4(η-C_5H_4)}(η^2-BH_4)], **2c**, in $C_6D_5CD_3$. Peaks due to the protons of the cyclopentadienyl rings are denoted * in the spectrum at 363 K.

nonbridged analogue [Nb(η-C_5H_5)$_2$(η^2-BH_4)].[12] The reduction in $\Delta G^{\ddagger}$ is smaller for the silicon- and ethylene-bridged species **2e** and **2c**,**d** (ca.12 kJ mol^{-1}). The data show that $\Delta G^{\ddagger}$ is most reduced when the *ansa*-bridge exerts a greater change in the geometry of the metallocene. To make a meaningful comparison between the values of $\Delta G^{\ddagger}$ for the various tetrahydroborate complexes, it is assumed that $\Delta S^{\ddagger}$ for the exchange process is essentially the same for all species. Furthermore it is assumed that exchange proceeds via the same mechanism in all cases.

Substitution of BD_4 for BH_4 does not appear to affect the barrier to exchange, as evidenced by the close similarity in $\Delta G^{\ddagger}$ for the compounds **2c** and **3c** and the compounds [Nb{(η-C_5H_4)CMe_2(η-C_5H_4)}(η^2-BH_4)] and **4**. Interestingly whereas $\Delta G^{\ddagger}$ is lower for the ethylene-bridged species **2c**,**d** relative to [Nb(η-C_5H_5)$_2$(η^2-BH_4)], in the vanadium compound **5** there is an increase in $\Delta G^{\ddagger}$ compared to [V(η-C_5H_5)$_2$(η^2-BH_4)]. However in both cases the change in $\Delta G^{\ddagger}$ is not as significant as that seen for the methylene-bridged species.

There is strong evidence that the bridge-terminal hydrogen exchange in group 5 metallocene tetrahy-

Table 3. Variable-Temperature ^{1}H NMR Spectroscopic Data for Group 5 Metallocene Tetrahydroborate Complexes

compound	T_c/K	δ_t/ppm	δ_b/ppm	$\delta_{b/t}$/ppm	ref
[Nb{(η-C_5H_4)CMe_2(η-C_5H_4)}(η^2-BH_4)]	228 ± 3[a]	5.2	−11.6	−3.4	*b*
[Nb{(η-C_5H_4)CMe_2(η-C_5H_4)}(η^2-BD_4)], **4**	198 ± 5[a]	5.3	−18.2	−3.0	*b*
[Nb{(η-C_5H_4)CEt_2(η-C_5H_4)}(η^2-BH_4)], **2a**	223 ± 3[a]	5.3	−11.6	−3.5	*b*
[Nb{(η-C_5H_4)C(C_5H_{10})(η-C_5H_4)}(η^2-BH_4)], **2b**	218 ± 3[a]	5.3	−11.5	−3.4	*b*
[Nb{(η-C_5H_4)C_2Me_4(η-C_5H_4)}(η^2-BH_4)], **2c**	308 ± 3[a]	5.3	−14.9	−5.0	*b*
[Nb{(η-C_5H_4)C_2Me_4(η-C_5H_4)}(η^2-BD_4)], **3c**	278 ± 5[a]	4.9	−15.3	−4.9	*b*
rac-[Nb{(η-$C_5H_3{}^tBu$)C_2Me_4(η-$C_5H_3{}^tBu$)}(η^2-BH_4)], **2d**	303 ± 3[a]	5.2	−13.9	−4.5	*b*
[Nb{(η-C_5H_4)$SiMe_2$(η-C_5H_4)}(η^2-BH_4)], **2e**	305 ± 3[a]	5.5	−14.9	−5.0	*b*
[Nb(η-C_5H_5)$_2$(η^2-BH_4)]	346 ± 3[c]	5.1	−16.2	−5.4	12
[Nb(η-C_5Me_5)$_2$(η^2-BH_4)]	388 ± 8[c]	5.2	−18.2	−7.0	12
[V{(η-C_5H_4)C_2Me_4(η-C_5H_4)}(η^2-BH_4)], **5**	263 ± 3[a]	4.8	−22.9	−9.1	*b*
[V(η-C_5H_5)$_2$(η^2-BH_4)]	186 ± 7[c]	5.0	−24.0	−9.5	18

[a] 500 MHz. [b] This work. [c] 90 MHz.

Table 4. Free Energy Barrier (at T_c) $\Delta G^{\ddagger}$ to Bridge-Terminal Hydrogen Exchange and Bending Angle β for Group 5 Metallocene Tetrahydroborate Complexes

compound	$\Delta G^{\ddagger}$/kJ mol^{-1}	β/deg	ref
[Nb{(η-C_5H_4)CMe_2(η-C_5H_4)}(η^2-BH_4)]	35.0 ± 1	114.1	*a*, 6
[Nb{(η-C_5H_4)CMe_2(η-C_5H_4)}(η^2-BD_4)], **4**	34.8 ± 2		*a*
[Nb{(η-C_5H_4)CEt_2(η-C_5H_4)}(η^2-BH_4)], **2a**	35.8 ± 1	115.6	*a*
[Nb{(η-C_5H_4)C(C_5H_{10})(η-C_5H_4)}(η^2-BH_4)], **2b**	35.0 ± 1		*a*
[Nb{(η-C_5H_4)C_2Me_4(η-C_5H_4)}(η^2-BH_4)], **2c**	49.9 ± 1	127.8	*a*
[Nb{(η-C_5H_4)C_2Me_4(η-C_5H_4)}(η^2-BD_4)], **3c**	49.1 ± 2		*a*
rac-[Nb{(η-$C_5H_3{}^tBu$)C_2Me_4(η-$C_5H_3{}^tBu$)}(η^2-BH_4)], **2d**	49.1 ± 1	124.7	*a*
[Nb{(η-C_5H_4)$SiMe_2$(η-C_5H_4)}(η^2-BH_4)], **2e**	49.3 ± 1	127.2	*a*
[Nb(η-C_5H_5)$_2$(η^2-BH_4)]	61.1 ± 1	127.1	12, 15
[Nb(η-C_5Me_5)$_2$(η^2-BH_4)]	68.6 ± 2		12
[V{(η-C_5H_4)C_2Me_4(η-C_5H_4)}(η^2-BH_4)], **5**	41.5 ± 1	132.3	*a*
[V(η-C_5H_5)$_2$(η^2-BH_4)]	31.8 ± 2		18

[a] This work.

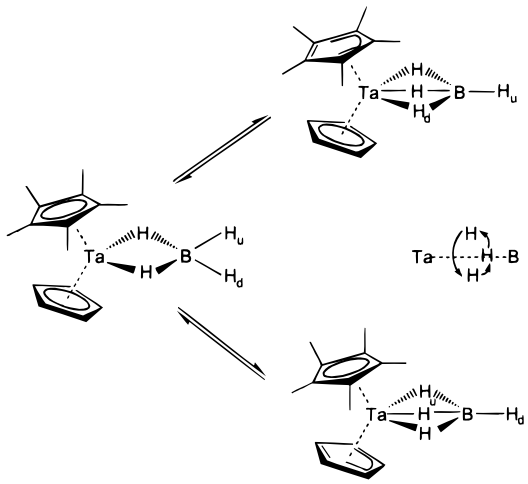

Figure 10. Proposed associative mechanism for exchange of bridging and terminal hydrogens in [Ta(η-C_5Me_5)(η-C_5H_5)(η^2-BH_4)].

droborate complexes occurs via an associative mechanism. A detailed 2D exchange NMR study of [Ta(η-C_5H_5)(η-C_5Me_5)(η^2-BH_4)] showed that there is negligible direct exchange between the terminal hydrogens.[11] A mechanism involving $\eta^5-\eta^3$ ring shift of one of the cyclopentadienyl rings upon coordination of a terminal hydrogen to the metal center in an η^3-BH_4 intermediate has been proposed (Figure 10). Either of these steps may be rate-limiting. Rotation of the coordinated η^3-BH_4 unit results in exchange of bridging and terminal hydrogens.

For a rate-limiting step involving a $\eta^5-\eta^3$ ring shift, a lower energetic barrier to hydrogen exchange would be expected when the strain imparted by the bridging unit is greatest. The degree of strain, as evidenced for example by the largest reduction in the bending angle β, is greatest for a single carbon-bridged metallocene such as the compound **2a**. It could be argued that a lower energetic barrier to formation of a η^3-BH_4 intermediate would be present when the metal center is opened up by a reduced bending angle β. Formation of a η^3-BH_4 intermediate involves stretching of a terminal B−H bond and, were this step rate-limiting, would be expected to display a kinetic isotope effect. We note that there was no apparent kinetic isotope effect on substitution of BD_4 for BH_4 for the compounds **2c** and **3c** and the compounds [Nb{(η-C_5H_4)CMe_2(η-C_5H_4)}(η^2-BH_4)] and **4**. On the evidence of the above structural and dynamic studies we suggest a rate-limiting $\eta^5-\eta^3$ ring shift of one of the cyclopentadienyl rings, followed by fast formation and rotation of an η^3-BH_4 intermediate.

Finally, that the IR data suggest a subtle weakening of the M−BH_4 covalent interaction as the bending angle β is decreased could also be significant with regard to the barrier to exchange.

Recent density functional calculations have shown that the position of the cyclopentadienyl rings relative to the metal has a significant effect on the frontier orbital structure of the metallocene.[19] It is anticipated that the change in orbital structure imposed by the presence of an *ansa*-bridge contributes to the differences in dynamic properties of the tetrahydroborate derivatives relative to the nonbridged systems. Energy profiles of possible hydrogen exchange mechanisms for bridged and nonbridged tetrahydroborate complexes are currently being investigated using density functional calculations.

In conclusion we have described the preparation of new *ansa*-metallocenes of group 5. For the tetrahy-

droborate derivatives the free energy barrier $\Delta G^{\ddagger}$ to bridge-terminal hydrogen exchange is considerably reduced relative to the nonbridged species when the *ansa*-bridge imposes a significant change in geometry in the metallocene.

Experimental Section

General Considerations. All manipulations of air- and/or moisture-sensitive materials were performed in an inert atmosphere using either a dual vacuum/nitrogen line and standard Schlenk techniques or in an inert atmosphere drybox containing nitrogen. Solvents were dried over the appropriate drying agent and distilled under nitrogen.

$NaBD_4$ and $LiBH_4$ were purchased from Aldrich and used as received. $NbCl_4$·2THF,[21] $[Li_2(C_5H_4)SiMe_2(C_5H_4)]$,[22] $[(MgCl)_2\{(C_5H_4)C_2Me_4(C_5H_4)\}$·4THF],[23] $[(MgCl)_2\{(C_5H_3{}^tBu)C_2Me_4(C_5H_3{}^tBu)\}$·4THF],[24] $[Nb\{(\eta\text{-}C_5H_4)CMe_2(\eta\text{-}C_5H_4)\}(\eta^2\text{-}BH_4)]$,[6] and $[V\{(\eta\text{-}C_5H_4)CMe_2(\eta\text{-}C_5H_4)\}Cl_2]$[9a] were prepared using standard literature methods. $[Li_2(C_5H_4)CEt_2(C_5H_4)]$ was prepared by the reaction between 6,6-diethylfulvene[25] and freshly distilled cyclopentadiene followed by deprotonation with *n*-butyllithium in a procedure analogous to that used to prepare $[Li_2(C_5H_4)CMe_2(C_5H_4)]$.[26]

The ^1H and ^{13}C NMR spectra were recorded using a Varian UNITY*plus* (^1H 500 MHz, ^{13}C 125 MHz) spectrometer and are at room temperature unless otherwise stated. Spectra were referenced internally using the residual protio solvent (^1H) and solvent (^{13}C) resonances relative to tetramethylsilane ($\delta = 0$ ppm). IR spectra were recorded on either a Mattson-Polaris or a Perkin-Elmer 1710 FT instrument. ESR spectra were recorded in CH_2Cl_2 on a Varian E 109 instrument and referenced to DPPH. Mass spectra (FAB) were performed by the EPSRC Mass Spectrometry Service at Swansea, U.K. Elemental analyses were performed by the Microanalytical Department of the Inorganic Chemistry Laboratory, Oxford.

Preparations. $[Nb\{(\eta\text{-}C_5H_4)CEt_2(\eta\text{-}C_5H_4)\}Cl_2]$, 1a. To a stirred suspension of $NbCl_4$·2THF (2.59 g, 6.83 mmol) in THF (50 cm^3) was added a solution of $[Li_2(C_5H_4)CEt_2(C_5H_4)]$ (1.45 g, 6.83 mmol) in THF (80 cm^3) over 1 h at room temperature. The resulting purple suspension was stirred overnight. Volatiles were removed under reduced pressure, and the resulting oily brown solid was extracted into toluene (3×50 cm^3). Toluene was removed under reduced pressure to leave crude $[Nb\{(\eta\text{-}C_5H_4)CEt_2(\eta\text{-}C_5H_4)\}Cl_2]$ (**1a**) as a dark brown solid. Yield = 0.9 g, 37%. An analytically pure sample of the compound **1a** was obtained by sublimation at 165 °C (10^{-1} mmHg).

$[Nb\{(\eta\text{-}C_5H_4)C(C_5H_{10})(\eta\text{-}C_5H_4)\}Cl_2]$, 1b. The two solids $NbCl_4$·2THF (4.0 g, 12.7 mmol) and $[Li_2(C_5H_4)C(C_5H_{10})(\eta^5\text{-}C_5H_4)]$ (2.86 g, 12.7 mmol) were stirred together in the absence of solvent to give a good admixture. Diethyl ether (80 cm^3) was added and the resulting brown suspension stirred for 3 days. The volatiles were removed under reduced pressure, and the resulting pale brown solid was Soxhlet extracted into dichloromethane over 5 h to yield a deep red/brown solution. Removal of volatiles under reduced pressure followed by washing with pentane (2×100 cm^3) yielded the compound $[Nb\{(\eta\text{-}C_5H_4)C(C_5H_{10})(\eta\text{-}C_5H_4)\}Cl_2]$ (**1b**) as a pale brown solid. Yield = 3.33 g, 70%.

The following compounds were prepared in an analogous manner to **1b**.

$[Nb\{(\eta\text{-}C_5H_4)C_2Me_4(\eta\text{-}C_5H_4)\}Cl_2]$, 1c: from $NbCl_4$·2THF and $[(MgCl)_2\{(C_5H_4)C_2Me_4(C_5H_4)\}$·4THF]. Yield = 2.86 g, 72%.

$[Nb\{(\eta\text{-}C_5H_3{}^tBu)C_2Me_4(\eta\text{-}C_5H_3{}^tBu)\}Cl_2]$, 1d: from $NbCl_4$·2THF and $[(MgCl)_2\{(C_5H_4)C_2Me_4(C_5H_3{}^tBu)\}$·4THF]. Yield of crude **1d** = 2.30 g, 74%. An analytically pure sample of the compound **1d** was obtained by sublimation at 160 °C (10^{-1} mmHg).

$[Nb\{(\eta\text{-}C_5H_4)SiMe_2(\eta\text{-}C_5H_4)\}Cl_2]$, 1e: from $NbCl_4$·2THF and $[Li_2(C_5H_4)SiMe_2(C_5H_4)]$. Yield = 0.8 g, 36%.

$[Nb\{(\eta\text{-}C_5H_4)CEt_2(\eta\text{-}C_5H_4)\}(\eta^2\text{-}BH_4)]$, 2a. A mixture of the compound **1a** (0.25 g, 0.69 mmol) and $LiBH_4$ (0.17 g, 7.9 mmol) was suspended in DME (40 cm^3) at room temperature. Effervescence was observed on addition of the solvent. The brown reaction mixture was stirred overnight, and then volatiles were removed under reduced pressure. The resulting solid was extracted into petroleum ether (bp 100−120 °C) (2×30 cm^3). This dark green solution was concentrated to 25 cm^3 and cooled to −80 °C, yielding the compound $[Nb\{(\eta\text{-}C_5H_4)CEt_2(\eta\text{-}C_5H_4)\}(\eta^2\text{-}BH_4)]$ (**2a**) as dark green crystals. Yield = 0.13 g, 62% (based on the compound **1a**).

The compounds **$[Nb\{(\eta\text{-}C_5H_4)C(C_5H_{10})(\eta\text{-}C_5H_4)\}(\eta^2\text{-}BH_4)]$** (**2b**) (yield = 0.04 g, 41%), **$[Nb\{(\eta\text{-}C_5H_4)C_2Me_4(\eta\text{-}C_5H_4)\}(\eta^2\text{-}BH_4)]$** (**2c**) (yield = 0.12 g, 70%), **$[Nb\{(\eta\text{-}C_5H_3{}^tBu)C_2Me_4(\eta\text{-}C_5H_3{}^tBu)\}(\eta^2\text{-}BH_4)]$** (**2d**) (yield = 0.09 g, 61%), and **$[Nb\{(\eta\text{-}C_5H_4)SiMe_2(\eta\text{-}C_5H_4)\}(\eta^2\text{-}BH_4)]$** (**2e**) (yield = 0.15 g, 66%) were prepared by the reaction of $LiBH_4$ with the corresponding dichlorides **1b**−**e**.

The compounds **$[Nb\{(\eta\text{-}C_5H_4)C_2Me_4(\eta\text{-}C_5H_4)\}(\eta^2\text{-}BD_4)]$** (**3c**) (yield = 0.04 g, 55%) and **$[Nb\{(\eta\text{-}C_5H_4)CMe_2(\eta\text{-}C_5H_4)\}(\eta^2\text{-}BD_4)]$** (**4**) (yield = 0.03 g, 41%) were prepared by the reaction of $NaBD_4$ with the compounds **1c** and $[Nb\{(\eta\text{-}C_5H_4)CMe_2(\eta\text{-}C_5H_4)\}Cl_2]$, respectively.

$[V\{(\eta\text{-}C_5H_4)C_2Me_4(\eta\text{-}C_5H_4)\}(\eta^2\text{-}BH_4)]$, 5. A green suspension of $[V\{(\eta\text{-}C_5H_4)C_2Me_4(\eta\text{-}C_5H_4)Cl_2\}]$ (0.15 g, 0.45 mmol) in DME (100 cm^3) at −30 °C was added to a flask charged with $NaBH_4$ (0.1 g, 2.6 mmol). The resulting violet suspension was stirred for 5 h while the temperature was maintained at −10 °C. The reaction mixture was filtered to give a violet solution. Removal of volatiles under reduced pressure yielded a pale violet solid, which was extracted into petroleum ether (bp 100−120 °C) (30 cm^3). The dark violet solution was cooled to −80 °C, yielding the compound $[V\{(\eta\text{-}C_5H_4)C_2Me_4(\eta\text{-}C_5H_4)\}(\eta^2\text{-}BH_4)]$ (**5**) as a dark violet crystalline solid. Yield = 0.09 g, 74%.

Crystal Structure Determination. Crystals of the compounds **2a**, **2c**−**e** (green), and **5** (violet) were grown from a petroleum ether (bp 100−120 °C) solution at ca. 193 K and isolated by filtration. A specimen was chosen under an inert atomsphere, covered with paratone-N oil, and mounted on the end of a glass fiber.

Data were collected at 150 K on an Enraf-Nonius DIP2000 image plate diffractometer with graphite-monochromated Mo Kα radiation ($\lambda = 0.71069$ Å). The images were processed with the DENZO[27] and SCALEPACK[28] programs. Corrections for Lorentz and polarization effects were performed.

All solution, refinement, and graphical calculations were performed using the CRYSTALS[29] and CAMERON[30] software packages. The crystal structures were solved by direct methods using the SIR92 program[31] and were refined by full-matrix least-squares procedures on *F*. All non-hydrogen atoms were

(21) Pedersen, S. F.; Hartung, J. B.; Roskamp, E. J.; Dragovich, P. S. *Inorg. Synth.* **1992**, *29*, 119.
(22) Bajgur, C. S.; Tikkanen, W. R.; Petersen, J. L. *Inorg. Chem.* **1985**, *24*, 2539−2546.
(23) Schwemlein, H.; Brintzinger, H. H. *J. Organomet. Chem.* **1983**, *254*, 69−73.
(24) Drewitt, M. J.; Barlow, S.; O'Hare, D.; Nelson, J. M.; Nguyen, P.; Manners, I. *J. Chem. Soc., Chem. Commun.* **1996**, 2153−2154.
(25) Stone, K. J.; Little, R. D. *J. Org. Chem.* **1984**, *49*, 1849−1853.
(26) Nifant'ev, I. E.; Ivchenko, P. V.; Borzov, M. V. *J. Chem. Res., Synop.* **1992**, 162.
(27) Otwinowski, Z. *DENZO*; Department of Molecular Biophysics and Biochemistry, Yale University: New Haven, CT, 1993.
(28) Otwinowski, Z.; Minor, W. *Methods Enzymol.* **1996**, *276*, 307−326.
(29) Watkin, D. J.; Prout, C. K.; Carruthers, J. R.; Betteridge, P. W. *CRYSTALS, Issue 10*; Chemical Crystallography Laboratory: Oxford, 1996.
(30) Watkin, D. J.; Prout, C. K.; Pearce, L. J. *CAMERON*; Chemical Crystallography Laboratory: Oxford, 1996.

Table 5. Crystallographic and Refinement Data for 2a, 2c−e, and 5

	2a	2c	2d	2e	5
formula	$C_{15}H_{22}NbB$	$C_{16}H_{24}NbB$	$C_{20}H_{40}NbB$	$C_{12}H_{18}NbBSi$	$C_{16}H_{24}VB$
fw	306.06	320.08	432.30	294.08	278.12
cryst size/mm^3	0.5 × 0.5 × 0.4	0.3 × 0.2 × 0.15	0.4 × 0.4 × 0.5	0.2 × 0.2 × 0.2	0.22 × 0.25 × 0.5
cryst syst	orthorhombic	triclinic	triclinic	monoclinic	triclinic
space group	$P2_12_12_1$	$P\bar{1}$	$P\bar{1}$	$P2_1/n$	$P\bar{1}$
a/Å	7.5850(6)	7.5840(2)	9.8890(3)	8.600(2)	7.4060(3)
b/Å	12.4240(6)	9.6590(4)	10.3510(3)	10.449(2)	9.6410(6)
c/Å	14.9090(7)	11.3790(4)	12.6830(4)	14.883(3)	11.3520(8)
α/deg		98.334(2)	96.689(2)		98.190(3)
β/deg		105.989(2)	108.360(2)	101.662(2)	106.382(4)
γ/deg		107.886(2)	108.838(2)		107.820(3)
V/Å^3	1405.0	738.19	1131.2	1305.8	716.7
Z	4	2	2	4	2
T/K	125	100	125	150	150
ρ/g cm^{-3}	1.45	1.44	1.27	1.50	1.29
abs coeff μ/mm^{-1}	0.80	0.76	0.51	0.94	0.65
no. of reflns	7259	6498	6621	7764	4099
no. of unique reflns	1540	2844	4262	2782	2626
no. of params[a]	166	259	247	148	175
R^b	0.0304	0.0179	0.0353	0.0355	0.0369
$R_w{}^b$	0.0315	0.0206	0.0615	0.0459	0.0386
R_{int}	0.031	0.012	0.060	0.024	0.018
goodness of fit	0.7562	1.0515	1.1695	0.6076	0.9038
largest final shift	0.000107	0.002569	0.006258	0.00675	0.000690
resid dens/e Å^3	0.33, −0.63	0.38, −0.50	0.88, −0.82	0.45, −0.47	0.36, −0.29

[a] Criterion for observation $I > 3\sigma(I)$. [b] $R = [\sum(|F_o| - |F_c|)/\sum|F_o|]$. $R_w = [\sum w(F_o^2 - F_c^2)^2/\sum w(F_o^2)^2]^{1/2}$.

refined with anisotropic displacement parameters. All carbon-bound hydrogen atoms were generated and allowed to ride on their corresponding carbon atoms with fixed thermal parameters. Hydrogen atoms bound to boron were located in the final difference map and their positions refined. A Chebychev weighting scheme with the parameters 1.84, −0.409, and 0.930 (**2a**), 1.45, 0.293, and 0.737 (**2c**), 1.94, 0.472, and 1.35 (**5**) or a statistical weighting scheme (**2d** and **2e**) was applied.

The crystallographic and refinement data are summarized in Table 5.

Acknowledgment. We thank the EPSRC for a studentship (to S.L.J.C.) and St. John's College, Oxford, for a Junior Research Fellowship (to L.H.D.). We are also grateful to Dr. Leigh H. Rees for assistance with X-ray crystallography.

Supporting Information Available: Complete tables of bond distances, bond angles, anisotropic thermal parameters, and fractional atomic coordinates for the compounds **2a**, **2c**−**e**, and **5**. This material is available free of charge via the Internet at http://www.pubs.acs.org.

OM990810N

(31) Altomare, A.; Cascarano, G.; Giacovazzo, C.; Guagliardi, A.; Burla, M. C.; Polidori, G.; Camalli, M. *J. Appl. Crystallogr., Sect. A* **1994**, *27*, 435.